



Available online at www.sciencedirect.com



Procedia Computer Science 00 (2022) 1–20

**Procedia
Computer
Science**

Abstract

The Hybrid High Order (HHO) method is a powerful discretization method which has only been recently applied from to non linear computational mechanics.

The Hybrid High Order method divides the domain of interest in cells of arbitrary polyhedral shape, whose boundaries is called the skeleton, and introduces two kinds of degrees of freedom: the displacements in the cell and the displacements of the skeleton.

Most introductory materials to the HHO method is focus on the mathematical aspects of the methods. While those aspects are important, an approach based on physical considerations would help spreading this method to the computational mechanics and engineering communities.

This paper derives Hybrid High Order method from the classical Hu–Washizu functional.

Practical implementation of the method is discussed in depth using notations closed to the ones used in standard finite elements textbooks, highlighting the use of polyhedral cells and the use of approximation spaces based on polynomials of arbitrary orders.

From the point of view of numerical performances, the elimination of the cell degrees of freedom is mandatory to reduce the size of the stiffness matrix. The standard static condensation, is presented, as well as a novel strategy called "cell equilibrium". Advantages and disadvantages of both strategies are discussed.

The resolution of axi-symmetrical problems, which has seldom, if ever, been discussed in the literature, is then presented.

Numerical examples prove the robustness of the method with regards to volumetric locking....

© 2011 Published by Elsevier Ltd.

Keywords:

Computational mechanics, Hybrid High Order method, Static condensation, Cell equilibrium algorithm, Volumetric locking, Axi-symmetric modelling hypothesis

1. Introduction

The origin of DG methods dates back to the pioneering work of [1], where an hyperbolic formualtion is used to solve the neutron transport equation.

2. The model problem

2.1. The standard Hu–Washizu lagragian

This paragraph introduces the standard Hu–Washizu three field principle. For the sake of simplicity, and without loss of generality, we consider the case of an hyperelastic material. Extensions to mechanical behaviours with internal state variables is treated in classical textbooks of computational mechanics. We will treat this extension in the Section 6 discussing the numerical implementation of the Hybrid High Order method and in Section 7 which provides several examples in plasticity.

2.1.1. Description of the mechanical problem and notations

Solid body. Let us consider a solid body whose reference configuration is denoted Ω . At a given time $t > 0$, the body is in the current configuration Ω_t .

Mechanical loading. The body is assumed to be submitted to a body force f_v acting in Ω_t , a prescribed displacement \mathbf{u}_d on the Dirichlet boundary $\partial_d\Omega_t$, and a contact load \mathbf{t}_n on the Neumann boundary $\partial_n\Omega_t$.

Deformation. The transformation mapping Φ takes a point from the reference configuration Ω to the current configuration Ω_t such that

$$\Phi(\mathbf{X}) = \mathbf{x} = \mathbf{X} + \mathbf{u}(\mathbf{X}) \quad (1)$$

where \mathbf{X} , \mathbf{x} and \mathbf{u} denote respectively the position in the reference configuration Ω , the position in the current configuration Ω_t and the displacement.

Deformation gradient, gradient of the displacement. The deformation gradient \mathbf{F} is defined as

$$\mathbf{F} = \nabla \Phi = \mathbf{I} + \mathbf{G} \quad (2)$$

where ∇ is the gradient operator in the reference configuration and

$$\mathbf{G} = \nabla \mathbf{u} \quad (3)$$

denotes the gradient of the displacement.

Stress tensor. The body is assumed made of an hyperelastic material described by a free energy ψ_Ω which relates the deformation gradient \mathbf{F} and the first Piola-Kirchhoff stress tensor \mathbf{P} such that

$$\mathbf{P} = \frac{\partial \psi_\Omega}{\partial \mathbf{F}} \quad (4)$$

2.1.2. Primal problem and Principle of Virtual Works

Total lagrangian. The total Lagrangian L_Ω^{VW} of the body is defined as the stored energy minus the work of external loadings, as follows:

$$L_\Omega^{VW} = \int_{\Omega} \psi_\Omega(\mathbf{F}(\mathbf{u})) - \int_{\Omega} \mathbf{f}_v \cdot \mathbf{u} - \int_{\partial_N \Omega} \mathbf{t}_N \cdot \mathbf{u}|_{\partial_N \Omega} \quad (5)$$

where the body forces \mathbf{f}_v and conctat tractions \mathbf{t}_N in the reference configuration have been obtained from their counterparts \mathbf{f}_v and \mathbf{t}_n using the Nanson formulae.

Principle of Virtual Works. The displacement \mathbf{u} satisfying the mechanical equilibrium minimizes the Lagragian L_Ω^{VW} . The first order variation of Lagrangian is given by:

$$\frac{\partial L_\Omega^{VW}}{\partial \mathbf{u}} (\delta \mathbf{u}) = \int_{\Omega} \mathbf{P} : \nabla \delta \mathbf{u} - \int_{\Omega} \mathbf{f}_v \cdot \delta \mathbf{u} - \int_{\partial_N \Omega} \mathbf{t}_N \cdot \delta \mathbf{u}|_{\partial_N \Omega} \quad (6)$$

which must be null for the the solution displacement. The solution displacement thus satisfies the principle of virtual work:

$$\int_{\Omega} \mathbf{P} : \nabla \delta \mathbf{u} = \int_{\Omega} \mathbf{f}_v \cdot \delta \mathbf{u} + \int_{\partial_N \Omega} \mathbf{t}_N \cdot \delta \mathbf{u}|_{\partial_N \Omega} \quad \forall \delta \mathbf{u}$$

2.1.3. The Hu-Washizu Lagrangian

The Hu-Washizu Lagrangian L_{Ω}^{HW} generalizes the previous variational principle by considering that the gradient of the displacement \mathbf{G} and the first Piola-Kirchoff \mathbf{P} stress are independent unknowns of the problem, such that:

$$L^{HW} = \int_{\Omega} \psi_{\Omega}(\mathbf{I} + \mathbf{G}) + (\nabla \mathbf{u} - \mathbf{G}) : \mathbf{P} - \int_{\Omega} \mathbf{f}_V \cdot \mathbf{u} - \int_{\partial_N \Omega} \mathbf{t}_N \cdot \mathbf{u}|_{\partial_N \Omega} \quad (7)$$

The solution $(\mathbf{u}, \mathbf{G}, \mathbf{P})$ satisfying the mechanical equilibrium minimizes the Lagragian L_{Ω}^{HW} . The first order variation of the Hu-Washizu Lagragian with respect to \mathbf{u} , \mathbf{G} , and \mathbf{P} yields

$$\frac{\partial L_{\Omega}^{HW}}{\partial \mathbf{u}}(\delta \mathbf{u}) = \int_{\Omega} \mathbf{P} : \nabla \delta \mathbf{u} - \int_{\Omega} \mathbf{f}_V \cdot \delta \mathbf{u} - \int_{\partial_N \Omega} \mathbf{t}_N \cdot \delta \mathbf{u}|_{\partial_N \Omega} \quad \forall \delta \mathbf{u} \quad (8a)$$

$$\frac{\partial L_{\Omega}^{HW}}{\partial \mathbf{P}}(\delta \mathbf{P}) = \int_{\Omega} (\nabla \mathbf{u} - \mathbf{G}) : \delta \mathbf{P} \quad \forall \delta \mathbf{P} \quad (8b)$$

$$\frac{\partial L_{\Omega}^{HW}}{\partial \mathbf{G}}(\delta \mathbf{G}) = \int_{\Omega} \left(\frac{\partial \psi}{\partial \mathbf{G}} - \mathbf{P} \right) : \delta \mathbf{G} \quad \forall \delta \mathbf{G} \quad (8c)$$

where equation (8b) and (8c) account for (3) and (4) respectively in a weak sense.

Practical importance of the Hu-Washizu principle. En continue, aucun intérêt. Par contre, très puissant une fois les bases d'approximations choisies.

Many variants:

- Ne considérer uniquement l'espace sphérique.
- Gardez des champs globaux: U-P-G inconnues nodales. Variantes liées aux choix des espaces d'approximations de U, P et G (Al-Akrass).
- Travailler par éléments: Assumed strain (c.f. Belytchko).

3. Introduction to discontinuous methods through a Hu-Washizu formulation

Many numerical methods consider a partition of the body into elementary parts.

In this section one considers a subpart T of the body Ω . This subpart is in equilibrium with the rest of the body $\Omega \setminus T$ if the displacements and the normal traction are continuous at the boundary of ∂T .

Enforcing the displacement continuity at the interface leads to so-called conformal methods, to which the standard finite element methods belongs.

On the contrary, this condition can be weakened by introducing an elastic interface of negligible size between T and $\Omega \setminus T$. This is the basis of Discontinuous Galerkin methods.

In this paper, we consider HDG and HHO methods where two elastic interfaces are introduced: one between T and its boundary ∂T and a second one between $\Omega \setminus T$ and ∂T .

Following this idea, we show in this section how the use of the Hu-Hashizu Lagrangian allows to recover the main ingredients of the HDG/HHO methods, namely the reconstructed gradient and the stabilisation operator.

3.1. Element description

Element geometry. In the following, the cell T is assumed to be convex. It is split into a core part $K \subset T$ with boundary ∂K , and into an interface part $I \subset T$ with boundary $\partial I = \partial K \cup \partial T$, as shown in Figure 1. The interface I has some thickness $\ell > 0$ that is supposed to be small compared to h_T the diameter of T . From a geometrical standpoint, the core par of the element K is an homotethy of T by some ratio inferior to 1.

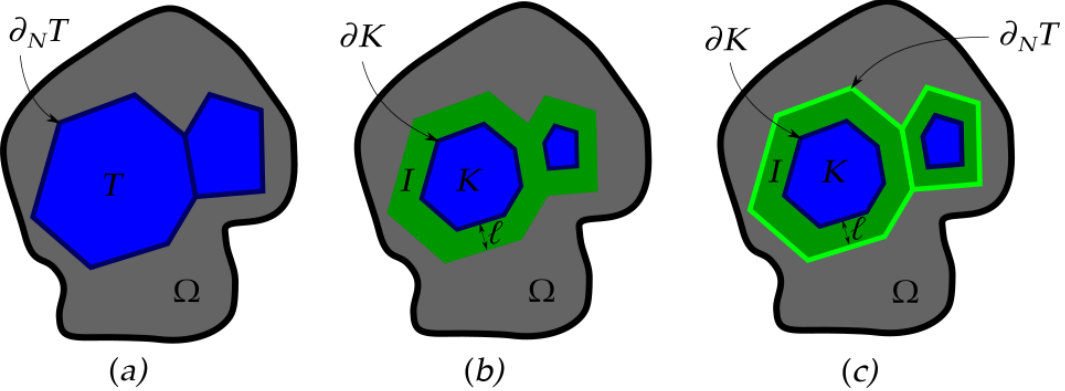


Figure 1. schematic representation of the composite region

Element behaviour. The core of the element K is made out of the same material that composes Ω and behaves according to the free energy potential ψ_Ω . The interface I is made out of a linear elastic-like material of Young modulus $\beta(\ell/h_T)$ with a zero Poisson ratio and its behavior is defined by the free energy potential ψ_I such that

$$\psi_I = \frac{1}{2} \beta \frac{\ell}{h_T} \nabla \mathbf{u}_I : \nabla \mathbf{u}_I \quad (9)$$

where the dimensionless ratio ℓ/h_T balances the accumulated energy with the size of the domain T .

Element loading. The core K is subjected to the volumetric loading \mathbf{f}_V , and to the contact load applied by the interface I onto ∂K . By continuity of the traction force, the same opposite contact load acts on I . The interface I is also subjected to some contact load $\mathbf{t}_{\partial NT}$ acting on ∂T , that accounts for the action of the rest of the solid Ω onto T .

Displacement, displacement gradient and stress fields. Let note \mathbf{u}_K the displacement field, \mathbf{G}_K the displacement gradient field and \mathbf{P}_K the stress field in K . Similarly, let \mathbf{u}_I the displacement field, \mathbf{G}_I the displacement gradient field and \mathbf{P}_I the stress field in I . The displacement of the boundary ∂T is denoted $\mathbf{u}_{\partial T}$. By continuity of the displacement field between K and ∂T , the displacement \mathbf{u}_I verifies

$$\mathbf{u}_I|_{\partial K} = \mathbf{u}_K|_{\partial K} \quad (10a)$$

$$\mathbf{u}_I|_{\partial T} = \mathbf{u}_{\partial T} \quad (10b)$$

Hu-Washizu Lagrangian of the element. By combining both the Lagrangian of the core K and that of the interface I , one obtains the total Lagrangian L_T^{HW} over the element such that

$$L_T^{HW} = \int_K \psi_\Omega + (\nabla_X \mathbf{u}_K - \mathbf{G}_K) : \mathbf{P}_K + \int_I \psi_I + (\nabla_X \mathbf{u}_I - \mathbf{G}_I) : \mathbf{P}_I - \int_K \mathbf{f}_V \cdot \mathbf{u}_K - \int_{\partial NT} \mathbf{t}_{\partial NT} \cdot \mathbf{u}_{\partial T} \quad (11)$$

3.2. Hypotheses

Since the interface is of negligible volume compared to that of the core, let make some assumptions on the displacement and the stress in the interface.

Displacement in the interface. The displacement in the interface I is assumed to be linear with respect to \mathbf{n} , such that its gradient is homogeneous in I

$$\nabla \mathbf{u}_I = \frac{\mathbf{u}_{\partial T} - \mathbf{u}_K|_{\partial K}}{\ell} \otimes \mathbf{n} \quad (12)$$

That is, the displacement of the interface I linearly bridges that of the boundary ∂T to that of the bulk K .

Stress in the interface. Furthermore, let assume that $\tilde{\mathbf{P}}_I$ is constant along the direction \mathbf{n} in I . By continuity of the traction force across ∂K , the following equality holds true

$$(\tilde{\mathbf{P}}_I - \tilde{\mathbf{P}}_K|_{\partial K}) \cdot \mathbf{n} = 0 \quad \text{in } I \quad (13)$$

3.3. Deriving the formulation of Hybrid discontinuous methods from the Hu-Washizu functional on the element

Using the hypotheses stated Section 3.2 on the displacement field and the stress field in I , one can write (11) as a term depending on the width of the interface ℓ and on the core and boundary unknowns only. The reader can refer to Section 8 for more details.

Simplified Hu–Washizu Lagrangian for a vanishing interface. In particular, making the width of the interface $\ell \rightarrow 0$, such that I vanishes and the core part K identifies to T , one obtains the simplified Hu–Washizu Lagrangian

$$\begin{aligned} J_T^{HW} = & \int_T \psi_\Omega + (\nabla \mathbf{u}_T - \mathbf{G}_T) : \tilde{\mathbf{P}}_T + \int_{\partial T} (\mathbf{u}_{\partial T} - \mathbf{u}_T|_{\partial T}) \cdot \tilde{\mathbf{P}}_T|_{\partial T} \cdot \mathbf{n} + \int_{\partial T} \frac{\beta}{2h_T} \|\mathbf{u}_{\partial T} - \mathbf{u}_T|_{\partial T}\|^2 \\ & - \int_T \mathbf{f}_V \cdot \mathbf{u}_T - \int_{\partial_N T} \mathbf{t}_{\partial_N T} \cdot \mathbf{u}_{\partial T} \end{aligned} \quad (14)$$

which fully defines the equilibrium of an element for discontinuous methods.

Hybridization of the primal unknown; the HDG and HHO methods. Since the interface I has vanished by making $\ell \rightarrow 0$, both $\mathbf{u}_T|_{\partial T}$ the trace of the displacement of the core part T onto ∂T and the displacement of the boundary $\mathbf{u}_{\partial T}$ coexist on ∂T . The displacement of the element T is thus said to be *hybrid*, and is denoted by the pair $(\mathbf{u}_T, \mathbf{u}_{\partial T})$.

The special case of DG methods. Replacing $\mathbf{u}_{\partial T}$ by $\mathbf{u}_{T'}|_{\partial T}$ for any neighboring cell T' amounts to describe the framework of Discontinuous Galerkin methods, where only the core unknown \mathbf{u}_T is considered, and the displacement jump on ∂T depends on $\mathbf{u}_{T'}|_{\partial T}$ the trace of the displacement of neighboring cells instead.

Conformal Galerkin formulation. By strongly enforcing continuity of the displacement across ∂T such that $\mathbf{u}_T|_{\partial T} = \mathbf{u}_{\partial T}$, one recovers the system defined in (7), which defines the framework of conformal methods.

Mixed problem for the discontinuous framework. The Lagrangian (14) defines the mixed field functional to minimize, which amounts to solve the system

$$\frac{\partial J_T^{HW}}{\partial \mathbf{u}_T} \delta \mathbf{u}_T = \int_T \tilde{\mathbf{P}}_T : \nabla \delta \mathbf{u}_T - \int_T \mathbf{f}_V \cdot \delta \mathbf{u}_T - \int_{\partial T} \boldsymbol{\theta}_{\partial T} \cdot \delta \mathbf{u}_T|_{\partial T} \quad \forall \delta \mathbf{u}_T \quad (15a)$$

$$\frac{\partial J_T^{HW}}{\partial \mathbf{u}_{\partial T}} \delta \mathbf{u}_{\partial T} = \int_{\partial_N T} (\boldsymbol{\theta}_{\partial T} - \mathbf{t}_{\partial_N T}) \cdot \delta \mathbf{u}_{\partial T} \quad \forall \delta \mathbf{u}_{\partial T} \quad (15b)$$

$$\frac{\partial J_T^{HW}}{\partial \mathbf{G}_T} \delta \mathbf{G}_T = \int_T \left(\frac{\partial \psi_\Omega}{\partial \mathbf{G}_T} - \tilde{\mathbf{P}}_T \right) : \delta \mathbf{G}_T \quad \forall \delta \mathbf{G}_T \quad (15c)$$

$$\frac{\partial J_T^{HW}}{\partial \tilde{\mathbf{P}}_T} \delta \tilde{\mathbf{P}}_T = \int_T (\nabla \mathbf{u}_T - \mathbf{G}_T) : \delta \tilde{\mathbf{P}}_T + \int_{\partial T} (\mathbf{u}_{\partial T} - \mathbf{u}_T|_{\partial T}) \cdot \delta \tilde{\mathbf{P}}_T|_{\partial T} \cdot \mathbf{n} \quad \forall \delta \tilde{\mathbf{P}}_T \quad (15d)$$

where we introduced the *reconstructed traction force* $\boldsymbol{\theta}_{\partial T} = \tilde{\mathbf{P}}_T|_{\partial T} \cdot \mathbf{n} + (\beta/h_T)(\mathbf{u}_{\partial T} - \mathbf{u}_T|_{\partial T})$. In particular, (15a) is the expression of the principle of virtual works in T , where the *reconstructed traction force* $\boldsymbol{\theta}_{\partial T}$ replaces the usual expression $\tilde{\mathbf{P}}_T \cdot \mathbf{n}$ in the external contribution. (15b) denotes a supplementary equation to the usual continuous problem as described in (8), to account for the continuity of the flux $\boldsymbol{\theta}_{\partial T}$ across the cell boundary. (15c) accounts for the constitutive equation in a weak sense, and (15d) defines the equation of an enhanced gradient field, that does not reduce to the projection of $\nabla \mathbf{u}_T$ as in (8c), since it is enriched by a boundary component that depends on the displacement jump, which is at the origin of the robustness of non-conformal methods to volumetric locking (see Section 8).

3.4. Problem in primal form

Reconstructed gradient. Since minimization of (15d) defines a linear problem with any displacement pair $(\mathbf{v}_T, \mathbf{v}_{\partial T})$, one can eliminate (15d) from the system (15). The resulting equation defines the so-called *reconstructed gradient* $\tilde{\mathbf{G}}_T(\mathbf{v}_T, \mathbf{v}_{\partial T})$ associated with any displacement pair $(\mathbf{v}_T, \mathbf{v}_{\partial T})$, that solves

$$\int_T \tilde{\mathbf{G}}_T(\mathbf{v}_T, \mathbf{v}_{\partial T}) : \boldsymbol{\tau}_T = \int_T \nabla \mathbf{v}_T : \boldsymbol{\tau}_T + \int_{\partial T} (\mathbf{v}_{\partial T} - \mathbf{v}_T|_{\partial T}) \cdot \boldsymbol{\tau}_T|_{\partial T} \cdot \mathbf{n} \quad \forall \boldsymbol{\tau}_T \in S(T) \quad (16)$$

Stress tensor. Likewise, one eliminates (15c) from (15). Assuming that the space of kinematically admissible stress fields is included in that of kinematically admissible displacement gradient fields, one considers the equality in a strong sense

$$\tilde{\mathbf{P}}_T = \frac{\partial \psi_\Omega}{\partial \tilde{\mathbf{G}}_T} \quad (17)$$

Total Lagrangian for the problem in primal form. By elimination of both (15c) and (15d) from (15), the functional for the problem in primal form (18) arises from (14)

$$J_T^{VW} = \int_T \psi_\Omega + \int_{\partial T} \frac{\beta}{2h_T} \|\mathbf{u}_{\partial T} - \mathbf{u}_T|_{\partial T}\|^2 - \int_T \mathbf{f}_V \cdot \mathbf{u}_T - \int_{\partial_N T} \mathbf{t}_{\partial_N T} \cdot \mathbf{u}_{\partial T} \quad (18)$$

Principle of virtual works for HDG methods. Minimization of the Lagrangian (18) amounts to find the displacement pair $(\mathbf{u}_T, \mathbf{u}_{\partial T})$ that solves

$$\delta J_{T,\text{int}}^{VW}((\mathbf{u}_T, \mathbf{u}_{\partial T}), (\delta \mathbf{u}_T, \delta \mathbf{u}_{\partial T})) - \delta J_{T,\text{ext}}^{VW}(\delta \mathbf{u}_T, \delta \mathbf{u}_{\partial T}) = 0 \quad \forall (\delta \mathbf{u}_T, \delta \mathbf{u}_{\partial T}) \quad (19)$$

with

$$\delta J_{T,\text{int}}^{VW} = \int_T \tilde{\mathbf{P}}_T(\tilde{\mathbf{G}}_T(\mathbf{u}_T, \mathbf{u}_{\partial T})) : \tilde{\mathbf{G}}_T(\delta \mathbf{u}_T, \delta \mathbf{u}_{\partial T}) + \int_{\partial T} (\beta/h_T) \mathbf{Z}_{\partial T}(\mathbf{u}_T, \mathbf{u}_{\partial T}) \cdot \mathbf{Z}_{\partial T}(\delta \mathbf{u}_T, \delta \mathbf{u}_{\partial T}) \quad (20a)$$

$$\delta J_{T,\text{ext}}^{VW} = \int_{\partial_N T} \mathbf{t}_{\partial_N T} \cdot \delta \mathbf{u}_{\partial T} + \int_T \mathbf{f}_V \cdot \delta \mathbf{u}_T \quad (20b)$$

where we introduced the jump function $\mathbf{Z}_{\partial T}$ such that

$$\mathbf{Z}_{\partial T}(\mathbf{v}_T, \mathbf{v}_{\partial T}) = \mathbf{v}_{\partial T} - \mathbf{v}_T|_{\partial T} \quad \forall (\mathbf{v}_T, \mathbf{v}_{\partial T}) \in U(\bar{T}) \quad (21)$$

In particular, one can readily see the resemblance of (20) with (6), where the so called *reconstructed gradient* $\tilde{\mathbf{G}}_T(\mathbf{u}_T, \mathbf{u}_{\partial T})$ plays the role of the usual displacement Lagrangian gradient $\nabla \mathbf{u}_T$, and where an additional *stabilization term* corresponding to a traction energy on the boundary has been added to account for the penalization of the displacement jump on ∂T through $\mathbf{Z}_{\partial T}$ (or, equivalently, to account for the infinitésimale interface that lays between the bulk domain and its boundary). Equations (18), (16) and (17) define the mechanical problem to solve at the cell level for Hybrid Discontinuous Galerkin methods, and (19) describes the weak form of these equations.

3.5. Small strain hypothesis extension

La formulation proposée en grandes déformations permet également un passage naturel au cadre des petites déformations. Dans ce contexte, étant donné que le gradient de la transformation $\tilde{\mathbf{F}}_T$ est supposé petit devant $\mathbf{1}$, on cherche le champ de déformation infinitésimale $\tilde{\boldsymbol{\varepsilon}}_T$ comme la formulation faible de $\nabla^s \mathbf{u}_T$ plutôt que le gradient du champ de déplacement $\tilde{\mathbf{G}}_T$. Le tenseur des contraintes $\tilde{\mathbf{P}}_T$ est alors identifié à $\tilde{\boldsymbol{\sigma}}_T$, de sorte que le problème (14) devient

$$\begin{aligned} J_T^{HW} = & \int_T \psi_\Omega + (\nabla^s \mathbf{u}_T - \tilde{\boldsymbol{\varepsilon}}_T) : \tilde{\boldsymbol{\sigma}}_T + \int_{\partial T} (\mathbf{u}_{\partial T} - \mathbf{u}_T|_{\partial T}) \cdot \tilde{\boldsymbol{\sigma}}_T|_{\partial T} \cdot \mathbf{n} + \int_{\partial T} \frac{\beta}{2h_T} \|\mathbf{u}_{\partial T} - \mathbf{u}_T|_{\partial T}\|^2 \\ & - \int_T \mathbf{f}_V \cdot \mathbf{u}_T - \int_{\partial_N T} \mathbf{t}_{\partial_N T} \cdot \mathbf{u}_{\partial T} \end{aligned} \quad (22)$$

En poursuivant le même développement que précédemment, l'énergie à minimiser est donnée par l'équation 18 comme dans le cadre des grandes déformations. En revanche, l'équation du gradient reconstruit 16 devient

$$\int_T \underline{\varepsilon}_T(\boldsymbol{v}_T, \boldsymbol{v}_{\partial T}) : \underline{\tau}_T = \int_T \nabla^s \boldsymbol{v}_T : \underline{\tau}_T + \int_{\partial T} (\boldsymbol{v}_{\partial T} - \boldsymbol{v}_T|_{\partial T}) \cdot \underline{\tau}_T|_{\partial T} \cdot \mathbf{n} \quad \forall \underline{\tau}_T \quad (23)$$

En particulier, les déformations $\underline{\varepsilon}_T$ étant symétriques, tout comme la contrainte $\underline{\sigma}_T$, on cherche donc ces grandeurs dans l'espace des déformations $G(T)$ et contraintes $S(T)$ statiquement admissibles et symétriques. L'expression de la contrainte en fonction de la déformation de cellule est alors donnée par

$$\underline{\sigma}_T = \frac{\partial \psi_\Omega}{\partial \underline{\varepsilon}_T} \quad (24)$$

4. Discretization

In this section, we specify the nature of the mesh, and introduce the so-called *skeleton* of the mesh, that bears boundary displacement unknowns. We then devise the problem to solve at the structural level, from the equilibrium of an element as described in Section 3.4. Approximation spaces for unknowns of the global problem are then described, which leads to several choices in terms of definition of the stabilization. Depending on such a choice, one recovers either the HDG method, or the HHO one. Finally, we give the expression of the global problem in discrete form.

4.1. Spatial discretization

Faces and skeleton of the mesh. The boundary ∂T of each element is decomposed in faces, such that a face F is a subset of Ω , and either there are two cells T and T' such that $F = \partial T \cap \partial T'$ (F is then an interior face), or there is a single cell T such that $F = \partial T \cap \partial\Omega$ (F is then an exterior face). For any cell T , let $\mathcal{F}(T) = \{F \in \mathcal{F} \mid F \subset \partial T\}$ the set of faces composing the boundary of T . Let finally $\mathcal{F}(\Omega) = \{F_i \subset \Omega \mid 1 \leq i \leq N_F\}$ the skeleton of the mesh, collecting all element faces F_i in the mesh, where N_F denotes the number of faces.

Mesh. Likewise, one defines the collection of all cells in the mesh as $\mathcal{T}(\Omega) = \{T_i \subset \Omega \mid 1 \leq i \leq N_T\}$, where N_T denotes the total number of cells. The composition of both $\mathcal{T}(\Omega)$ and $\mathcal{F}(\Omega)$ forms the hybrid mesh $\tilde{\mathcal{T}}(\Omega) = \{\mathcal{T}(\Omega), \mathcal{F}(\Omega)\}$.

4.2. Global continuous problem

Global unknown. Let the global unknown $(\boldsymbol{v}_T, \boldsymbol{v}_F)$ a displacement pair such that for each $T \in \mathcal{T}(\Omega)$, $\boldsymbol{v}_T = \boldsymbol{v}_T$ in T and for each $F \in \mathcal{F}(\Omega)$, $\boldsymbol{v}_F = \boldsymbol{v}_F$ on F , where \boldsymbol{v}_T and \boldsymbol{v}_F denote a cell and a face displacement field respectively.

Global weak form. The weak form of the global mechanical problem of Ω reads : find the global displacement unknown pair $(\boldsymbol{u}_T, \boldsymbol{u}_F)$ verifying $\boldsymbol{u}_F|_{\partial_D \Omega} = \boldsymbol{u}_D$ on $\partial_D \Omega$ such that $\forall (\delta \boldsymbol{u}_T, \delta \boldsymbol{u}_F)$

$$\delta J_{\mathcal{T},\text{int}}^{VW} - \delta J_{\mathcal{T},\text{ext}}^{HW} = 0 \quad (25)$$

with

$$\delta J_{\mathcal{T},\text{int}}^{VW} = \sum_{T \in \mathcal{T}(\Omega)} \int_T \mathbf{P}_T(\mathbf{G}_T(\boldsymbol{u}_T, \boldsymbol{u}_{\partial T})) : \mathbf{G}_T(\delta \boldsymbol{u}_T, \delta \boldsymbol{u}_{\partial T}) + \int_{\partial T} (\beta/h_T) \mathbf{Z}_{\partial T}(\boldsymbol{u}_T, \boldsymbol{u}_{\partial T}) \cdot \mathbf{Z}_{\partial T}(\delta \boldsymbol{u}_T, \delta \boldsymbol{u}_{\partial T}) \quad (26a)$$

$$\delta J_{\mathcal{T},\text{ext}}^{HW} = \sum_{F \in \mathcal{F}_N(\Omega)} \int_F \mathbf{t}_N \cdot \delta \boldsymbol{u}_F + \sum_{T \in \mathcal{T}(\Omega)} \int_T \mathbf{f}_V \cdot \delta \boldsymbol{u}_T \quad (26b)$$

where for each element $T \in \mathcal{T}(\Omega)$, the boundary displacement field $\boldsymbol{v}_{\partial T}$ is such that $\boldsymbol{v}_{\partial T} = \boldsymbol{v}_F$ on F for every $F \in \mathcal{F}(T)$

4.3. Functional discretization and stabilization

Discrete functional space. For each element $T \in \mathcal{T}(\Omega)$, we denote $U^h(T)$ the approximation displacement space in the cell, and $V^h(\partial T)$ that on the boundary. Similarly, let $G^h(T)$ the space used to build the discrete reconstructed gradient and $S^h(T)$ that chosen for the discrete stress such that

$$\begin{aligned} U^h(T) &= P^l(T, \mathbb{R}^d) \\ V^h(\partial T) &= P^k(\partial T, \mathbb{R}^d) \\ G^h(T) &= P^k(T, \mathbb{R}^{d \times d}) \\ S^h(T) &= P^k(T, \mathbb{R}^{d \times d}) \end{aligned}$$

where the cell displacement polynomial order l might be chosen different from the face displacement order k such that $k - 1 \leq l \leq k + 1$.

HDG stabilization. Accounting for the possible different polynomial order between the cell and faces, one can specify a discrete jump function in a natural way such that it delivers the displacement difference point-wise for any displacement pair $(\mathbf{v}_T^l, \mathbf{v}_{\partial T}^k) \in U^h(\bar{T})$

$$\mathbf{Z}_{\partial T}^{HDG}(\mathbf{v}_T^l, \mathbf{v}_{\partial T}^k) = \Pi_{\partial T}^k(\mathbf{v}_{\partial T}^k - \mathbf{v}_T^l|_{\partial T}) \quad (27)$$

where $U^h(\bar{T}) = U^h(T) \times V^h(\partial T)$ and $\Pi_{\partial T}^k$ denotes the orthogonal projector onto $V^h(\partial T)$. This straightforward discrete jump function is at the origin of Hybrid Discontinuous Galerkin methods, and grants a convergence of order k in the energy norm.

HHO stabilization. A richer discrete jump function $\mathbf{Z}_{\partial T}^{HHO}$ providing a convergence of order $k + 1$ in the energy norm was introduced in [2], hence giving the Hybrid High Order method its name, such that

$$\mathbf{Z}_{\partial T}^{HHO}(\mathbf{v}_T^l, \mathbf{v}_{\partial T}^k) = \Pi_{\partial T}^k(\mathbf{v}_{\partial T}^k - \mathbf{v}_T^l|_{\partial T} - ((I_T^{k+1} - \Pi_T^k)(\mathbf{w}_T^{k+1}))|_{\partial T}) \quad (28)$$

where Π_T^k is the projector onto $P^k(T, \mathbb{R}^d)$, I_T^{k+1} is the identity function in $D^h(T) = P^{k+1}(T, \mathbb{R}^d)$.

Reconstructed higher order displacement. The term \mathbf{w}_T^{k+1} in (28) denotes a higher order discrete displacement in $D^h(T)$ that solves for any displacement pair $(\mathbf{v}_T^l, \mathbf{v}_{\partial T}^k) \in U^h(\bar{T})$

$$\int_T \nabla \mathbf{w}_T^{k+1} : \nabla \mathbf{d}_T^{k+1} = \int_T \nabla \mathbf{v}_T^l : \nabla \mathbf{d}_T^{k+1} + \int_{\partial T} (\mathbf{v}_{\partial T}^k - \mathbf{v}_T^l) \cdot \nabla \mathbf{d}_T^{k+1} \cdot \mathbf{n} \quad \forall \mathbf{d}_T^{k+1} \in D^h(T) \quad (29a)$$

$$\int_T \mathbf{w}_T^{k+1} = \int_T \mathbf{v}_T^l \quad (29b)$$

4.4. Global discrete problem

Discrete global approximation spaces. Let $U^h(\mathcal{T}) = \prod_{T \in \mathcal{T}(\Omega)} U^h(T)$ the global discrete cell displacement space. Let $V^h(\mathcal{F}) = \prod_{F \in \mathcal{F}(\Omega)} V^h(F)$ the global discrete face displacement space, and $U^h(\bar{\mathcal{T}}) = U^h(\mathcal{T}) \times V^h(\mathcal{F})$ the global unknown approximation space. Similarly, let $U_0^h(\mathcal{T})$ and $V_0^h(\mathcal{F})$ the respective discrete mesh and skeleton virtual displacement spaces, and $U_0^h(\bar{\mathcal{T}}) = U_0^h(\mathcal{T}) \times V_0^h(\mathcal{F})$ the discrete virtual global displacement space.

Discrete global problem. The global problem in discrete form writes : find the pair $(\mathbf{u}_T^l, \mathbf{u}_{\mathcal{F}}^k) \in U^h(\bar{\mathcal{T}})$ verifying $\mathbf{u}_{\mathcal{F}}^k|_{\partial_D \Omega} = \mathbf{u}_D$ on $\partial_D \Omega$ such that $\forall (\delta \mathbf{u}_T^l, \delta \mathbf{u}_{\mathcal{F}}^k) \in U_0^h(\bar{\mathcal{T}})$

$$\delta J_{\mathcal{T}, \text{int}}^{HHO} - \delta J_{\mathcal{T}, \text{ext}}^{HHO} = 0 \quad (30)$$

with

$$\delta J_{\mathcal{T}, \text{int}}^{HHO} = \sum_{T \in \mathcal{T}(\Omega)} \int_T \mathbf{P}_T^k(\mathbf{G}_T^k(\mathbf{u}_T^l, \mathbf{u}_{\partial T}^k)) : \mathbf{G}_T^k(\delta \mathbf{u}_T^l, \delta \mathbf{u}_{\partial T}^k) + \int_{\partial T} (\beta/h_T) \mathbf{Z}_{\partial T}^{HHO}(\mathbf{u}_T^l, \mathbf{u}_{\partial T}^k) \cdot \mathbf{Z}_{\partial T}^{HHO}(\delta \mathbf{u}_T^l, \delta \mathbf{u}_{\partial T}^k) \quad (31a)$$

$$\delta J_{\mathcal{T}, \text{ext}}^{HHO} = \sum_{F \in \mathcal{F}_N(\Omega)} \int_F \mathbf{t}_N \cdot \delta \mathbf{u}_F^k + \sum_{T \in \mathcal{T}(\Omega)} \int_T \mathbf{f}_V \cdot \delta \mathbf{u}_T^l \quad (31b)$$

where the discrete reconstructed gradient $\tilde{\mathbf{G}}_T^k(\mathbf{v}_T^l, \mathbf{v}_{\partial T}^k) \in G^h(T)$ solves $\forall (\mathbf{v}_T^l, \mathbf{v}_{\partial T}^k) \in U^h(\bar{T})$

$$\int_T \tilde{\mathbf{G}}_T^k(\mathbf{v}_T^l, \mathbf{v}_{\partial T}^k) : \boldsymbol{\tau}_T^k = \int_T \nabla \mathbf{v}_T^l : \boldsymbol{\tau}_T^k + \int_{\partial T} (\mathbf{v}_{\partial T}^k - \mathbf{v}_T^l|_{\partial T}) \cdot \boldsymbol{\tau}_T^k |_{\partial T} \cdot \mathbf{n} \quad \forall \boldsymbol{\tau}_T^k \in S^h(T) \quad (32)$$

5. A HHO method for the axi-symmetric framework

In the following section, we devise a Hybrid High order method for an axi-symmetric framework. In such a framework, owing to geometrical assumptions on the displacement and its gradient, the definition of the reconstructed gradient (16) and of that of the higher order displacement (29) needs be modified accordingly. Details about the definitions of these ingredients can be found in Section 8. Moreover, owing to

Axi-symmetric framework. The cartesian space is expressed in cylindrical coordinates and a point $X \in \Omega$ has coordinates $X = (r, z, \theta)$ where r denotes the radial component, z the ordinate one, and θ is the angular component describing a revolution around the axis $r = 0$. By cylindrical symmetry, the angular displacement u_θ is supposed to be zero, and both components u_r and u_z do not depend on the angular coordinate θ .

Cell displacement gradient. The partial derivatives of \mathbf{u}_T with respect to the cylindrical coordinates are given by

$$\forall i, j \in \{r, z\}, u_{Ti,j} = \frac{\partial u_{Ti}}{\partial j} \quad \text{and} \quad u_{T\theta,\theta} = \frac{u_{Tr}}{r} \quad (33)$$

Axis faces treatment. Since in cylindrical coordinates, all integrals depend on the radial component r , boundary integrals vanish at $r = 0$ on the symmetry axis. Therefore, the reconstructed gradient (and the stabilization) do not depend on a closed surface wrapping a T located on the symmetry axis. However, this feature is necessary to prove the robustness of the HHO method to volumetric locking (see Section 8). Therefore, we exclude the symmetry axis from the domain, by considering infinitely thin cylindrical faces of radius $\varrho > 0$ surrounding it (see Figure 2).

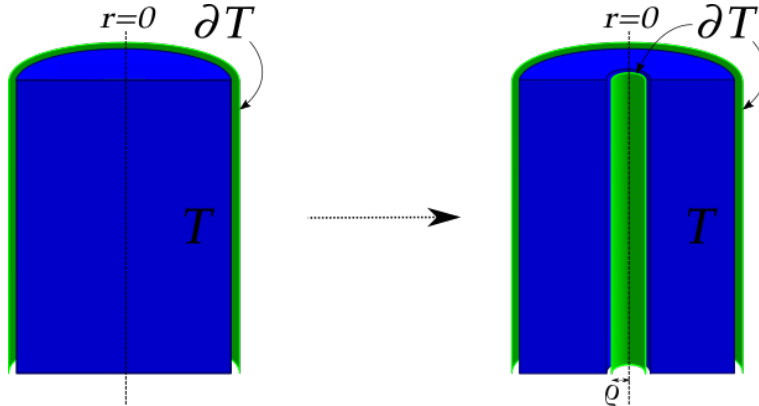


Figure 2. schematic representation of the modeling of a face located on the symmetry axis

6. Implementation

In this section, we specify the underlying matricial implementation of problem (31). In the following, the expression $\{\cdot\}$ denotes a real-valued vector, and the notation $[\cdot]$ a real-valued matrix.

Quadrature. As is customary with finite element methods, integrals are evaluated numerically by means of a quadrature rule on an element shape. Hence, let Q_T a quadrature rule for the cell T of order at least $2k$. A quadrature point is denoted X_q and a quadrature weight w_q .

6.1. Reconstructed gradient and stabilization operators

Reconstructed gradient operator. From an algebraic standpoint, (32) defines a linear problem consisting in inverting a mass matrix in $G^h(T)$. One can thus define $[B_T]$ the discrete gradient operator acting on the pair $(\mathbf{v}_T^l, \mathbf{v}_{\partial T}^k)$ at a quadrature point $\mathbf{x}_q \in Q_T$ to evaluate the discrete gradient $\tilde{\mathbf{G}}_T^k(\mathbf{v}_T^l, \mathbf{v}_{\partial T}^k)$ such that

$$\{\tilde{\mathbf{G}}_T^k(\mathbf{v}_T^l, \mathbf{v}_{\partial T}^k)\}(X_q) = [B_T](\mathbf{x}_q) \cdot \begin{Bmatrix} \mathbf{v}_T^l \\ \mathbf{v}_{\partial T}^k \end{Bmatrix} \quad \forall (\mathbf{v}_T^l, \mathbf{v}_{\partial T}^k) \in U^h(\bar{T}) \quad (34)$$

where $[B_T]$ is composed by a cell block B_T and a boundary block $B_{\partial T}$.

Stabilization operator. Similarly, the algebraic realization of (28) amounts to compute the stabilization operator $[Z_T]$ such that

$$\{\mathbf{Z}_{\partial T}^{HHO}(\mathbf{v}_T^l, \mathbf{v}_{\partial T}^k)\} = [Z_T] \cdot \begin{Bmatrix} \mathbf{v}_T^l \\ \mathbf{v}_{\partial T}^k \end{Bmatrix} \quad \forall (\mathbf{v}_T^l, \mathbf{v}_{\partial T}^k) \in U^h(\bar{T}) \quad (35)$$

as for $[B_T]$, the operator $[Z_T]$ is composed by a cell block Z_T and a boundary block $Z_{\partial T}$.

Offline computation. Since (32) and (28) depend on the geometry of the element T only, one can compute the operators $[B_T]$ and $[Z_T]$ for each element once and for all in an offline pre-computation step by working in the reference configuration. Once this offline step is performed, the algebraic form of the problem resembles closely to the standard finite element one, where the operator $[B_T]$ replaces the usual shape function gradient operator, and the stabilization operator $[Z_T]$ is incorporated in the expression of the tangent matrix and in that of internal forces.

6.2. Iterative method

Notations. In the following, let $(\mathbf{u}_T^{l,m,n}, \mathbf{u}_{\partial T}^{k,m,n})$ denote the displacement pair value at some pseudo time step m and some iteration n . The initial value of the displacement at time step $m = 0$ and iteration $n = 0$ is set to zero, and at a new pseudo time step $m + 1$, the displacement at the first iteration $n = 0$ takes the value of the displacement of the last iteration of the previous time step.

Internal forces. In such a context, the internal forces vector $\{F_T^{int}(\mathbf{u}_T^{l,m,n}, \mathbf{u}_{\partial T}^{k,m,n})\}$ writes

$$\{F_T^{int}(\mathbf{u}_T^{l,m,n}, \mathbf{u}_{\partial T}^{k,m,n})\} = \sum_{X_q \in Q_T} [B_T]^{\text{trans}}(X_q) \cdot \{\tilde{\mathbf{P}}_T^k(\tilde{\mathbf{G}}_T^k(\mathbf{u}_T^{l,m,n}, \mathbf{u}_{\partial T}^{k,m,n}))\}(X_q) + \frac{\beta}{h_T} [Z_T]^{\text{trans}} \cdot [Z_T] \cdot \begin{Bmatrix} \mathbf{u}_T^{l,m,n} \\ \mathbf{u}_{\partial T}^{k,m,n} \end{Bmatrix} \quad (36)$$

where the superscript $[\cdot]^{\text{trans}}$ denotes the transpose operation, and $\{\tilde{\mathbf{P}}_T^k(\tilde{\mathbf{G}}_T^k(\mathbf{u}_T^{l,m,n}, \mathbf{u}_{\partial T}^{k,m,n}))\}$ is the stress components vector, computed by integration of the behavior law at each quadrature point X_q from the values of the displacement gradient $\tilde{\mathbf{G}}_T^k(\mathbf{u}_T^{l,m,n}, \mathbf{u}_{\partial T}^{k,m,n})$.

External forces. The external forces vector is, as is customary with the standard finite element method, the evaluation of the given bulk and boundary loads at respective cell and face quadrature points tested against the respective cell and face shape functions, and is denoted

$$\{F_T^{ext}\} = \begin{Bmatrix} \mathbf{f}_V \\ \mathbf{t}_N \end{Bmatrix} \quad (37)$$

Tangent matrix. The tangent matrix $[K_T^{tan}(\mathbf{u}_T^{l,m,n}, \mathbf{u}_{\partial T}^{k,m,n})]$ is the sum of the usual product of the displacement gradients by the tangent operator $\tilde{\mathbf{A}}(\mathbf{u}_T^{l,m,n}, \mathbf{u}_{\partial T}^{k,m,n})$ and of an additional stabilization term such that

$$[K_T^{tan}(\mathbf{u}_T^{l,m,n}, \mathbf{u}_{\partial T}^{k,m,n})] = \sum_{X_q \in Q_T} [B_T]^{\text{trans}}(X_q) \cdot [\tilde{\mathbf{A}}(\mathbf{u}_T^{l,m,n}, \mathbf{u}_{\partial T}^{k,m,n})](X_q) \cdot [B_T](X_q) + \frac{\beta}{h_T} [Z_T]^{\text{trans}} \cdot [Z_T] \quad (38)$$

where $\tilde{\mathbf{A}}(\mathbf{u}_T^{l,m,n}, \mathbf{u}_{\partial T}^{k,m,n})$ is the derivative of the stress with respect to the displacement gradient

$$\tilde{\mathbf{A}}(\mathbf{u}_T^{l,m,n}, \mathbf{u}_{\partial T}^{k,m,n}) = \frac{\partial \tilde{\mathbf{P}}_T^k}{\partial \tilde{\mathbf{G}}_T^k} \quad (39)$$

Newton method. Following the iterative Newton method, the algebraic system to solve at the element level consists in finding the displacement increment $(\delta \mathbf{u}_T^l, \delta \mathbf{u}_{\partial T}^k)$ that solves

$$-\left[K_T^{tan}(\mathbf{u}_T^{l,m,n}, \mathbf{u}_{\partial T}^{k,m,n}) \right] \cdot \begin{Bmatrix} \delta \mathbf{u}_T^l \\ \delta \mathbf{u}_{\partial T}^k \end{Bmatrix} = \left\{ R_T^{m,n} \right\} \quad \text{with} \quad \left\{ R_T^{m,n} \right\} = \left\{ F_T^{int}(\mathbf{u}_T^{l,m,n}, \mathbf{u}_{\partial T}^{k,m,n}) \right\} - \left\{ F_T^{ext} \right\} \quad (40)$$

such that the displacement at the next iteration is incremented by the displacement increment $(\delta \mathbf{u}_T^l, \delta \mathbf{u}_{\partial T}^k)$

$$\begin{Bmatrix} \mathbf{u}_T^{l,m,n+1} \\ \mathbf{u}_{\partial T}^{k,m,n+1} \end{Bmatrix} = \begin{Bmatrix} \mathbf{u}_T^{l,m,n} \\ \mathbf{u}_{\partial T}^{k,m,n} \end{Bmatrix} + \begin{Bmatrix} \delta \mathbf{u}_T^l \\ \delta \mathbf{u}_{\partial T}^k \end{Bmatrix} \quad (41)$$

6.3. Static condensation

Static condensation. Since both $[B_T]$ and $[Z_T]$ are expressed in terms of cell and boundary blocks, so does the tangent matrix which can be decomposed into four coupled cell-boundary blocks with the notation

$$\left[K_T^{tan}(\mathbf{u}_T^{l,m,n}, \mathbf{u}_{\partial T}^{k,m,n}) \right] = \begin{bmatrix} K_{TT}(\mathbf{u}_T^{l,m,n}, \mathbf{u}_{\partial T}^{k,m,n}) & K_{T\partial T}(\mathbf{u}_T^{l,m,n}, \mathbf{u}_{\partial T}^{k,m,n}) \\ K_{\partial T T}(\mathbf{u}_T^{l,m,n}, \mathbf{u}_{\partial T}^{k,m,n}) & K_{\partial T \partial T}(\mathbf{u}_T^{l,m,n}, \mathbf{u}_{\partial T}^{k,m,n}) \end{bmatrix} \quad (42)$$

Moreover, since $\tilde{A}(\mathbf{u}_T^{l,m,n}, \mathbf{u}_{\partial T}^{k,m,n})$ is definite symmetric (and positive until an eventual loss of coercivity for e.g. high plastic deformations), the cell block K_{TT} is invertible and one can condense it through a Schur complement step in order to eliminate the cell unknown, such that (40) expresses only in terms of boundary increment unknowns

$$-\left[K_T^{tan}(\mathbf{u}_T^{l,m,n}, \mathbf{u}_{\partial T}^{k,m,n}) \right]_{\text{cond}} \cdot \left\{ \delta \mathbf{u}_{\partial T}^k \right\} = \left\{ F_T^{int}(\mathbf{u}_T^{l,m,n}, \mathbf{u}_{\partial T}^{k,m,n}) \right\}_{\text{cond}} - \left\{ F_T^{ext} \right\}_{\text{cond}} = \left\{ R_T^{m,n} \right\}_{\text{cond}} \quad (43)$$

with

$$\left[K_T^{tan} \right]_{\text{cond}} = \left[K_{\partial T \partial T} \right] - \left[K_{\partial T T} \right] \cdot \left[K_{TT} \right]^{-1} \cdot \left[K_{T\partial T} \right] \quad \text{and} \quad \left\{ R_T \right\}_{\text{cond}} = \left\{ R_{\partial T} \right\} - \left[K_{\partial T T} \right] \cdot \left[K_{TT} \right]^{-1} \cdot \left\{ R_T \right\} \quad (44)$$

and the incremental cell displacement expresses linearly with respect to the boundary one such that

$$\left\{ \delta \mathbf{u}_T^l \right\} = \left[K_{TT} \right]^{-1} \left(-\left\{ R_T \right\} - \left[K_{T\partial T} \right] \cdot \left\{ \delta \mathbf{u}_{\partial T}^k \right\} \right) \quad (45)$$

6.4. Algorithmic aspects

Linear static condensation algorithm. At a given pseudo-time step m and iteration n , the element displacement unknown is incremented by the element displacement increment. The reconstructed gradient field is then computed, and is used to integrate the behaviour law, which provides the stress and tangent operator values at quadrature points. The internal forces, external forces and tangent matrix are then computed, and condensed on the element faces. The resulting system is assembled on the global system matrix, and a new value of the increment is computed by inverting the global matrix. A schematic representation this procedure is given in Figure 3

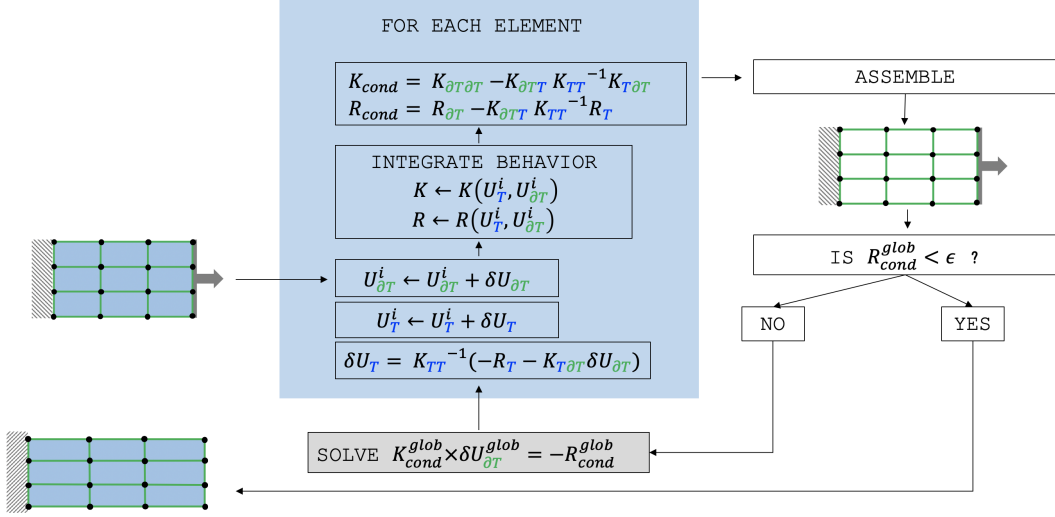


Figure 3. Description schématique de l'algorithme de condensation statique

Cell equilibrium algorithm. We propose an alternative to the static condensation solving algorithm, postulating an implicit relation between the increment of the cell unknowns and the increment of the faces, that consists in solving locally a nonlinear system on the cell increment at a fixed face increment. This non-linear local procedure adds up to the algorithm described above, to ensure the equilibrium of the cell with its faces at each iteration of the global problem. This new solution scheme is described in Figure 4, where we note i a Newton iteration for solving the global problem on the set of face unknowns, and j a Newton iteration for solving the local problem on the cell unknowns in an element.

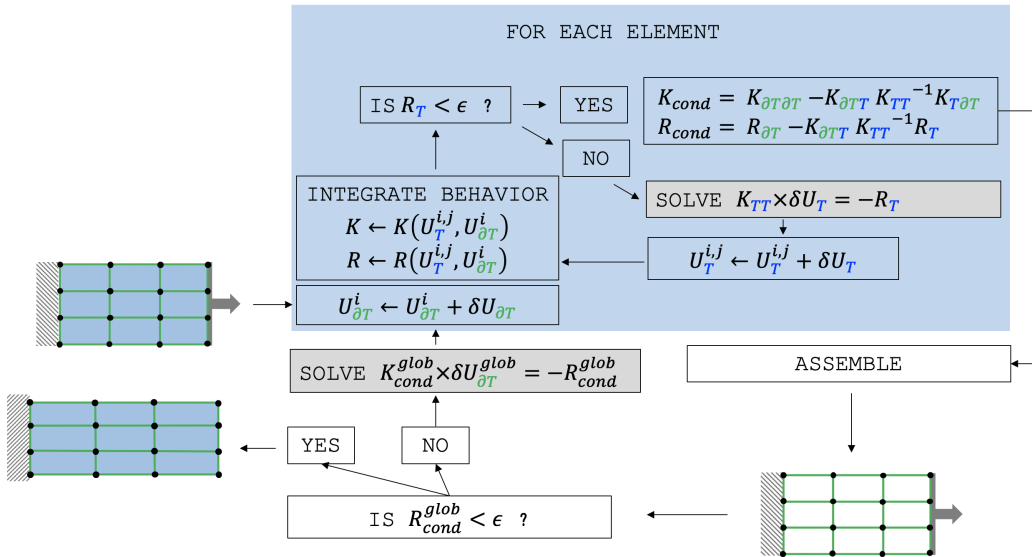


Figure 4. Description schématique de l'algorithme d'équilibre de cellule

We show in Section 7 that this algorithm gives identical results to those obtained with the Linear static condensation algorithm.

7. Numerical examples

In this section, we evaluate the proposed axi-symmetric HHO method on classical test cases taken from the literature to emphasize robustness to volumetric locking. In order to cover a wide scope of applications, we consider both the small and large strains framework, for linear elasticity and elasto-plastic behaviors. The first test case is that of a elasto-perfect plastic swelling sphere. The second one consists in the necking of a notched bar, and the third one consists in the swelling of an elastic hollow cylinder. In this section, we denote by $\text{HHO}(k, l)$ the HHO element of order k on faces, and order l in the cell.

7.1. Perfect plastic swelling sphere in small strains

In this section, we specify the thermodynamical framework in which falls the considered test case, *i.e.* that of elasto-plasticity under the small strain hypothesis. Then we describe the chosen behavior law for the numerical example, as well as the mechanical setting of the test case. Results are finally displayed and discussed at the end of the present section.

7.1.1. Plastic behavior in small strains

Dans le cadre de la thermodynamique des milieux continus, la combinaison de l'application des deux premiers principes de la thermodynamique donne lieu à l'équation de Clausius-Duhem qui postule la positivité de l'énergie de dissipation

$$\mathcal{D} = (\boldsymbol{\sigma}_T - \frac{\partial \psi_\Omega}{\partial \dot{\boldsymbol{\varepsilon}}_T}) : \dot{\boldsymbol{\varepsilon}}_T - \rho \frac{\partial \psi_\Omega}{\partial v_{int}} \dot{v}_{int} \geq 0 \quad (46)$$

en l'absence de dépendance du problème à la température. Dans le cadre de l'hyper-élasticité qui est un processus de transformation réversible, comme évoqué Section 2, l'ensemble V_{int} des variables internes v_{int} est supposé vide, de sorte que l'inégalité (46) revient à l'équation d'égalité (4). En revanche, pour des comportements dissipatifs de nature élasto-visco-plastique, on introduit un certains nombre de variables internes, qui sont liées à l'expression de l'énergie dissipée et à l'irréversibilité de la transformation. Pour des déformations infinitésimales, on suppose la décomposition additive de la déformation

$$\dot{\boldsymbol{\varepsilon}}_T = \dot{\boldsymbol{\varepsilon}}_T^e + \dot{\boldsymbol{\varepsilon}}_T^p \quad (47)$$

En une partie élastique $\dot{\boldsymbol{\varepsilon}}_T^e$ et une partie plastique $\dot{\boldsymbol{\varepsilon}}_T^p$. En particulier, dans le cadre des matériaux standards généralisés, on suppose l'existence d'un potentiel également décomposable en une partie élastique et en une partie plastique tel que

$$\psi_\Omega = \psi_\Omega^e(\boldsymbol{\varepsilon}_T^e) + \psi_\Omega^p(v_{int}) \quad (48)$$

Comme évoqué Section 2, le potentiel d'énergie libre de Helmholtz ψ_Ω dépend éventuellement d'un ensemble de variables internes v_{int} dans V_{int} , qui a été supposé vide jusque là. Dans le cadre d'un comportement élasto-visco-plastique, on introduit au moins une variable interne, de manière à assurer la positivité de l'énergie dissipée. Par injection de (48) dans (46), il vient que le tenseur des contraintes $\boldsymbol{\sigma}_T$ est la force duale associée aux déformations élastiques $\boldsymbol{\varepsilon}_T^e$. On définit également les forces thermodynamiques V_T duales des variables internes v_{int} telles que

$$\mathcal{D} = \boldsymbol{\sigma}_T : \dot{\boldsymbol{\varepsilon}}_T^p - \rho \frac{\partial \psi_\Omega}{\partial v_{int}} \dot{v}_{int} = \begin{Bmatrix} \boldsymbol{\sigma}_T \\ V_T \end{Bmatrix} \cdot \begin{Bmatrix} \dot{\boldsymbol{\varepsilon}}_T^p \\ \dot{v}_{int} \end{Bmatrix} \geq 0 \quad \text{with} \quad V_T = -\rho \frac{\partial \psi_\Omega}{\partial v_{int}} \quad (49)$$

Par ailleurs, le cadre des matériaux standards généralisés stipule l'existence d'un convex potential ϕ containing the origin, together with a threshold function f , that define the evolution of the generalized strains such that

$$\dot{v}_{int} = \frac{\partial \phi}{\partial f} \frac{\partial f}{\partial V_T} \quad (50)$$

Le potentiel ϕ dépend de la fonction de charge f telle que celle-ci contient l'origine, est différentiable en tout point de ...

En particulier, on introduit l'ensemble des variables internes $V_{int} = \{\varepsilon_T^p, p\}$ avec p la déformation plastique cumulée, et le potentiel plastique

$$\psi_\Omega^p(\varepsilon_T^p, p) = \frac{K}{2} \varepsilon_T^p : \varepsilon_T^p + \frac{K}{2} p^2 \quad (51)$$

où K est le module d'écrouissage cinématique, et H le module d'écrouissage isotrope. Les forces thermodynamiques associées aux variables internes ε_T^p et p sont respectivement $K\varepsilon_T^p$ et Hp .

$$f(\sigma_T^p, q) = \sqrt{\frac{3}{2}} \quad (52)$$

We introduce the discrete logarithmic stress tensor $\underline{\underline{E}} = 1/2\ln(\underline{\underline{F}}_T^t \cdot \underline{\underline{F}}_T)$

7.1.2. Perfect plastic swelling sphere

This benchmark consists in a quasi-incompressible sphere under uniform internal loading. This test case has an analytical solution and the state of the specimen is known when the plastic region has reached the external border of the sphere. The sphere has an inner radius $r_{int} = 0.8$ mm and an outer radius $r_{ext} = 1$ mm. An internal radial displacement u is imposed. The mesh is composed of XXX quadrangles (see Figure 6). The simulation is performed until the limit load corresponding to an internal displacement of 0.2 mm is reached.

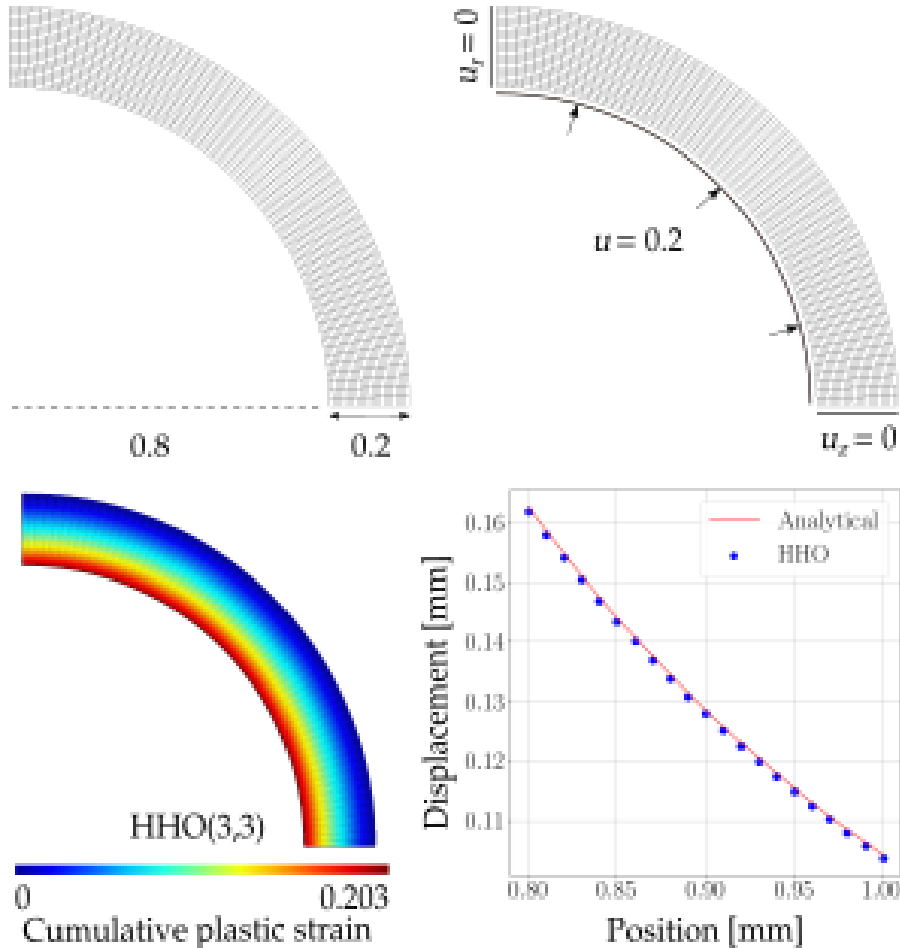


Figure 5. sphere

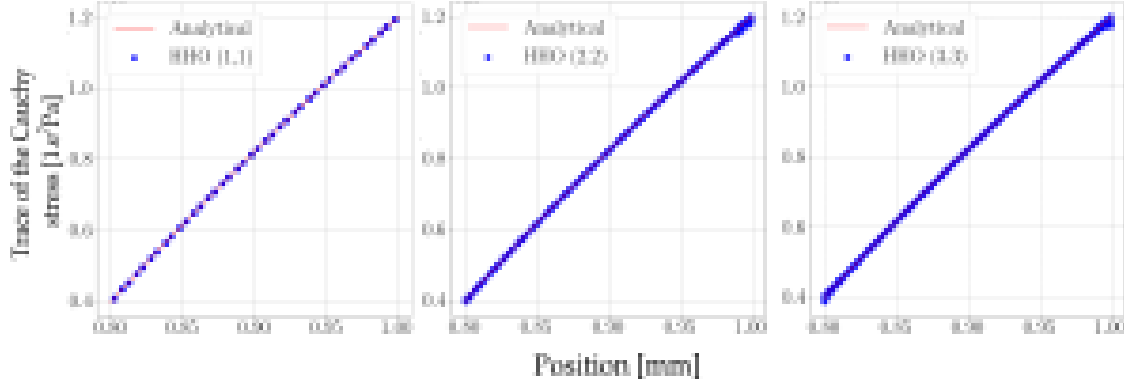


Figure 6. sphere

7.2. Necking of a notched bar

In this first benchmark, we consider a 2D rectangular bar with an initial imperfection. The bar is subjected to uniaxial extension. This example has been studied previously by many authors as a necking problem [3,5,7,8,22] and can be used to test the robustness of the different methods. The bar has a length of 53.334 mm and a variable width from an initial width value of 12.826 mm at the top to a width of 12.595 mm at the center of the bar to create a geometric imperfection. A vertical displacement $u_y = 5\text{mm}$ is imposed at both ends, as shown in Figure 2A. For symmetry reasons, only one-quarter of the bar is discretized, and the mesh is composed of 400 quadrangles (see Figure 2B). The load-displacement curve is plotted in Figure 2C. We observe that, except for Q1, all the other methods give very similar results. Moreover, the equivalent plastic strain p , respectively, the trace of the Cauchy stress tensor σ , are shown in Figure 3, respectively, in Figure 4, at the quadrature points on the final configuration. A sign of locking is the presence of strong oscillations in the trace of the Cauchy stress tensor σ . We notice that the cG formulations Q1 and Q2 lock, contrary to the HHO, Q2-RI, and UPG methods that deliver similar results. We remark, however, that the results for HHO(1;1), HHO(1;2), and Q2-RI are slightly less smooth than for HHO(2;2), HHO(2;3), and UPG. The reason is that, on a fixed mesh, the three former methods have less quadrature points than the three latter ones (see Table 1) (HHO(2;2), HHO(2;3), and UPG have the same number of quadrature points). Therefore, the stress is evaluated using less points in HHO(1;1), HHO(1;2), and Q2-RI. It is sufficient to refine the mesh or to increase the order of the quadrature by two in HHO(1;1) and HHO(1;2) to retrieve similar results to those for the three other methods (not shown for brevity).

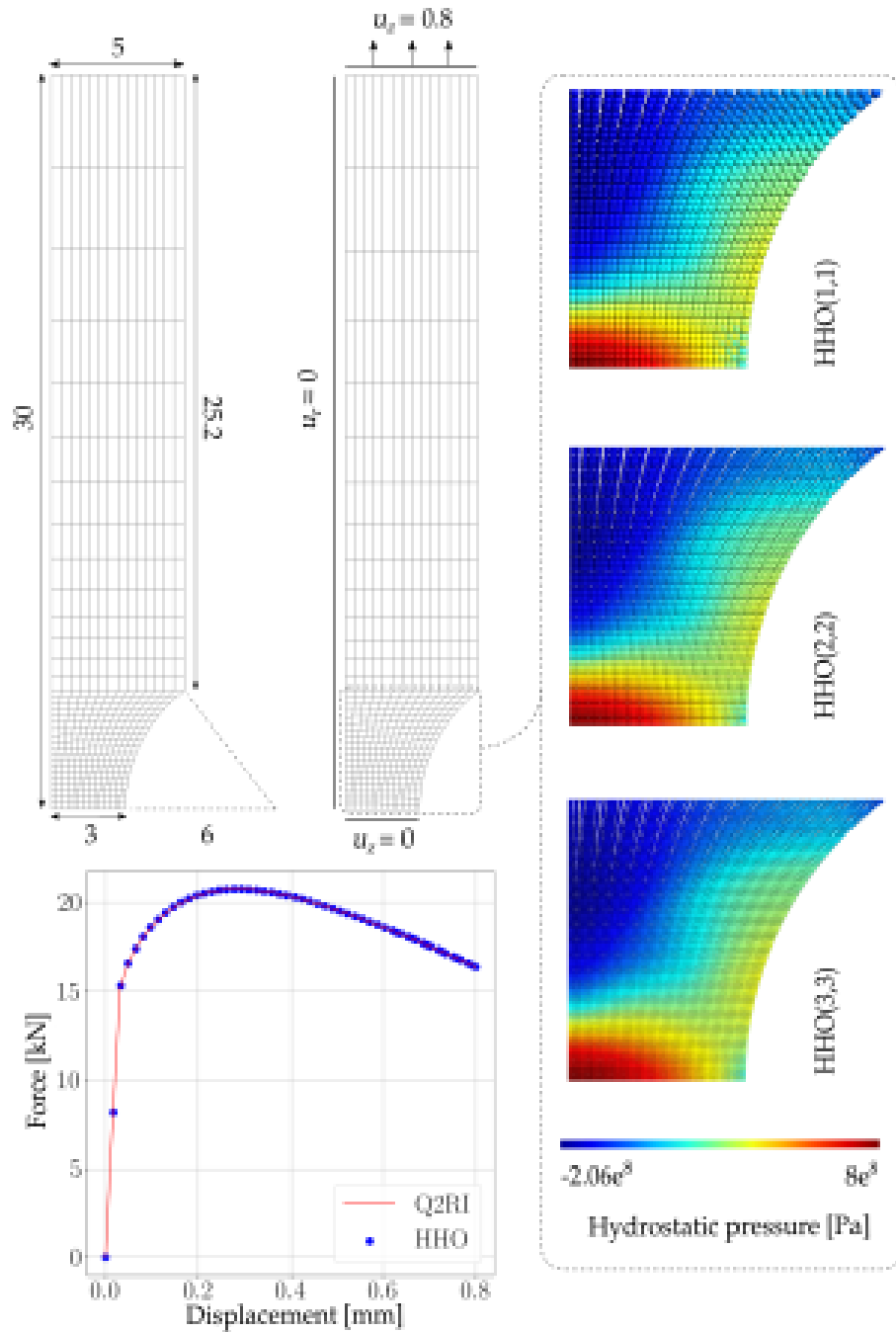


Figure 7. ssna

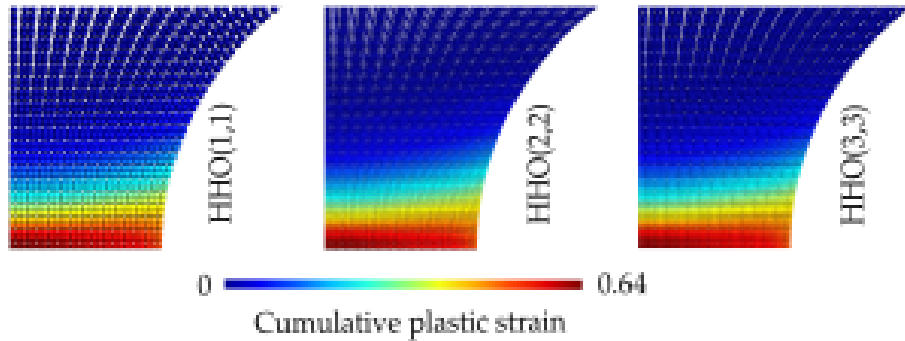


Figure 8. ssna

7.3. Quasi-incompressible sphere under internal pressure

This last benchmark 6 consists of a quasi-incompressible sphere under internal pressure for which an analytical solution is known when the entire sphere has reached a plastic state. This benchmark is particularly challenging compared to the previous ones since we consider here perfect plasticity. The sphere has an inner radius $R_{in} = 0.8$ mm and an outer radius $R_{out} = 1$ mm. An internal radial pressure P is imposed. For symmetry reasons, only one-eighth of the sphere is discretized, and the mesh is composed of 1580 tetrahedra (see Figure 10A). The simulation is performed until the limit load corresponding to an internal pressure 2.54 MPa is reached. The equivalent plastic strain p is plotted for HHO(1;2) in Figure 10B, and the trace of the Cauchy stress tensor σ is compared for HHO, UPG, and T2 methods in Figure 11 at all the quadrature points on the final configuration for the limit load. We notice that the quadratic element T2 locks, whereas HHO and UPG do not present any sign of locking and produce results that are very close to the analytical solution. However, the trace of the Cauchy stress tensor σ is slightly more dispersed around the analytical solution for HHO(2;2) and HHO(2;3) than for HHO(1;1) and HHO(1;2) near the outer boundary. For this test case, we do not expect that HHO(2;2) and HHO(2;3) will deliver more accurate solutions than HHO(1;1) and HHO(1;2) since the geometry is discretized using tetrahedra with planar faces. We next investigate the influence of the quadrature order k_Q on the accuracy of the solution. The trace of the Cauchy stress tensor σ is compared for HHO(1;1), HHO(2;2), and UPG methods in Figure 12 at all the quadrature points on the final configuration for the limit load, and for a quadrature order k_Q higher than the one employed in Figure 11 (HHO(1;2) and HHO(2;3) give similar results and are not shown for brevity). We remark that, when we increase the quadrature order, UPG locks for quasi-incompressible finite deformations, whereas HHO does not lock, and the results are (only) a bit more dispersed around the analytical solution. Moreover, HHO(2;2) is less sensitive than HHO(1;1) to the choice of the quadrature order k_Q . Note that this problem is not present for HHO methods with small deformations. Furthermore, this sensitivity to the quadrature order seems to be absent for finite deformations when the elastic deformations are compressible (the plastic deformations are still incompressible). To illustrate this claim, we perform the same simulations as before but for a compressible material. The Poisson ratio is taken now as $\nu = 0.3$ (recall that we used $\nu = 0.499$ in the quasi-incompressible case), whereas the other material parameters are unchanged. Unfortunately, an analytical solution is no longer available in the compressible case. We compare again the trace of the Cauchy stress tensor σ for HHO(1;1), HHO(2;2), and UPG methods in Figure 13 at all the quadrature points on the final configuration and for different quadrature orders k_Q . We observe a quite marginal dependence on the quadrature order for HHO methods (as in the quasi-incompressible case), whereas the UPG method still locks if the order of the quadrature is increased. Moreover, in the compressible case, HHO(2;2) gives a more accurate solution than HHO(1;1).

8. Appendix

$$\begin{aligned} J_{I,\text{int}}^{HW} &:= \int_I \psi_I + (\nabla \mathbf{u}_I - \mathbf{G}_I) : \mathbf{P}_I \\ &= (1 - \frac{\alpha}{2}\ell) \int_{\partial K} \frac{\beta}{2h_T} \|\mathbf{u}_{\partial T} - \mathbf{u}_K|_{\partial K}\|^2 + (1 - \frac{\alpha}{2}\ell) \int_{\partial K} (\mathbf{u}_{\partial T} - \mathbf{u}_K|_{\partial K}) \cdot \mathbf{P}_K|_{\partial K} \cdot \mathbf{n} - \int_I \mathbf{G}_I : \mathbf{P}_I \end{aligned} \quad (53)$$

The development of (53) is given in Appendix. Injecting (53) in (11) yields

$$\begin{aligned} J_T^{HW} &= \int_K \psi_\Omega + (\nabla \mathbf{u}_K - \mathbf{G}_K) : \mathbf{P}_K + (1 - \frac{\alpha}{2}\ell) \int_{\partial K} (\mathbf{u}_{\partial T} - \mathbf{u}_K|_{\partial K}) \cdot \mathbf{P}_K|_{\partial K} \cdot \mathbf{n} \\ &\quad + (1 - \frac{\alpha}{2}\ell) \int_{\partial K} \frac{\beta}{2h_T} \|\mathbf{u}_{\partial T} - \mathbf{u}_K|_{\partial K}\|^2 - \int_I \mathbf{G}_I : \mathbf{P}_I - \int_K \mathbf{f}_V \cdot \mathbf{u}_K - \int_I \mathbf{f}_V \cdot \mathbf{u}_I - \int_{\partial N_T} \mathbf{t}_{\partial N_T} \cdot \mathbf{u}_{\partial T} \end{aligned} \quad (54)$$

Development 8.1 (Interafce simplification). Let $C_I = \{v \in L^2(I) \mid v \cdot \mathbf{n} = \text{cste}\}$ the set of L^2 -functions which are constant along the normal axis in I . For any function in C_I , the following equality holds true:

$$\int_I v dV = \int_{\partial K} \int_{\epsilon=0}^{\ell} v(1 - \alpha\epsilon) dS d\epsilon = \ell(1 - \frac{\alpha}{2}\ell) \int_{\partial K} v dS \quad (55)$$

Noticing that $\nabla \mathbf{u}_I \in C_I$, one has :

$$\begin{aligned} \int_I \psi_I &= \ell(1 - \frac{\alpha}{2}\ell) \int_{\partial K} \frac{1}{2} \beta \frac{\ell}{h_T} \nabla \mathbf{u}_I : \nabla \mathbf{u}_I \\ &= \ell(1 - \frac{\alpha}{2}\ell) \int_{\partial K} \frac{\beta}{2\ell h_T} (\mathbf{u}_{\partial T} - \mathbf{u}_K|_{\partial K}) \otimes \mathbf{n} : (\mathbf{u}_{\partial T} - \mathbf{u}_K|_{\partial K}) \otimes \mathbf{n} \\ &= \ell(1 - \frac{\alpha}{2}\ell) \int_{\partial K} \frac{\beta}{2\ell h_T} \sum_{i,j} (u_{\partial T i} - u_{K i}|_{\partial K})^2 n_j^2 \\ &= \ell(1 - \frac{\alpha}{2}\ell) \int_{\partial K} \frac{\beta}{2\ell h_T} \sum_j n_j^2 \sum_i (u_{\partial T i} - u_{K i}|_{\partial K})^2 \\ &= \ell(1 - \frac{\alpha}{2}\ell) \int_{\partial K} \frac{\beta}{2\ell h_T} \sum_i (u_{\partial T i} - u_{K i}|_{\partial K})^2 \\ &= \ell(1 - \frac{\alpha}{2}\ell) \int_{\partial K} \frac{\beta}{2\ell h_T} \|\mathbf{u}_{\partial T} - \mathbf{u}_K|_{\partial K}\|^2 \\ &= (1 - \frac{\alpha}{2}\ell) \int_{\partial K} \frac{\beta}{2h_T} \|\mathbf{u}_{\partial T} - \mathbf{u}_K|_{\partial K}\|^2 \end{aligned} \quad (56)$$

Moreover, for \mathbf{P}_I in C_I :

$$\begin{aligned} \int_I \nabla \mathbf{u}_I : \mathbf{P}_I &= \ell(1 - \frac{\alpha}{2}\ell) \int_{\partial K} \nabla \mathbf{u}_I : \mathbf{P}_I \\ &= \ell(1 - \frac{\alpha}{2}\ell) \int_{\partial K} \frac{1}{\ell} (\mathbf{u}_{\partial T} - \mathbf{u}_K|_{\partial K}) \otimes \mathbf{n} : \mathbf{P}_K|_{\partial K} \\ &= \ell(1 - \frac{\alpha}{2}\ell) \int_{\partial K} \frac{1}{\ell} \sum_{i,j} (u_{\partial T i} - u_{K i}|_{\partial K}) n_j P_{Kij}|_{\partial K} \\ &= \ell(1 - \frac{\alpha}{2}\ell) \int_{\partial K} \frac{1}{\ell} (\mathbf{u}_{\partial T} - \mathbf{u}_K|_{\partial K}) \cdot \mathbf{P}_K|_{\partial K} \cdot \mathbf{n} \\ &= (1 - \frac{\alpha}{2}\ell) \int_{\partial K} (\mathbf{u}_{\partial T} - \mathbf{u}_K|_{\partial K}) \cdot \mathbf{P}_K|_{\partial K} \cdot \mathbf{n} \end{aligned} \quad (57)$$

And Finally :

$$J_{I,int}^{HW} = (1 - \frac{\alpha}{2}\ell) \int_{\partial K} \frac{\beta}{2h_T} \|\mathbf{u}_{\partial T} - \mathbf{u}_K|_{\partial K}\|^2 + (1 - \frac{\alpha}{2}\ell) \int_{\partial K} (\mathbf{u}_{\partial T} - \mathbf{u}_K|_{\partial K}) \cdot \mathbf{P}_K|_{\partial K} \cdot \mathbf{n} - \int_I \mathbf{G}_I : \mathbf{P}_I \quad (58)$$

Development 8.2 (Elliptic projection). Let $U^h(T) \subset U(T)$ and $U^\perp(T) \subset U(T)$ such that $U(T) = U^h(T) \oplus U^\perp(T)$, and set $\mathbf{u}_T = \mathbf{u}_T^h + \mathbf{u}_T^\perp$ with $\mathbf{u}_T^h \in U^h(T)$ and $\mathbf{u}_T^\perp \in U^\perp(T)$ the orthogonal projections of \mathbf{u}_T onto $U^h(T)$ and $U^\perp(T)$ respectively. Let $V^h(\partial T) \subset V(\partial T)$ and $\mathbf{u}_{\partial T}^h \in V^h(\partial T)$ the orthogonal projection of \mathbf{u}_T onto $V^h(\partial T)$. The orthogonal projection of \mathbf{u}_T onto $U^h(\bar{T}) = U^h(T) \times V^h(\partial T)$ is then the displacement pair $(\mathbf{u}_T^h, \mathbf{u}_{\partial T}^h)$. Let $S^h(T) = \{\boldsymbol{\tau}_T^h \in S(T) \mid \nabla \cdot \boldsymbol{\tau}_T^h \in U^h(T) \mid \boldsymbol{\tau}_T^h|_{\partial T} \cdot \mathbf{n} \in V^h(\partial T)\}$, and $\mathbf{G}_T^h \in S^h(T)$ the solution of (16) for $(\mathbf{u}_T^h, \mathbf{u}_{\partial T}^h)$ such that

$$\int_T \mathbf{G}_T^h(\mathbf{u}_T^h, \mathbf{u}_{\partial T}^h) : \boldsymbol{\tau}_T^h = \int_T \nabla \mathbf{u}_T^h : \boldsymbol{\tau}_T^h + \int_{\partial T} (\mathbf{u}_{\partial T}^h - \mathbf{u}_T^h|_{\partial T}) \cdot \boldsymbol{\tau}_T^h|_{\partial T} \cdot \mathbf{n} \quad \forall \boldsymbol{\tau}_T^h \in S^h(T) \quad (59)$$

using the fact that $\mathbf{u}_{\partial T}^h$ is the projection of \mathbf{u}_T onto $V^h(\partial T)$ and that $\boldsymbol{\tau}|_{\partial T} \cdot \mathbf{n} \in V^h(\partial T)$:

$$\begin{aligned} \int_T \mathbf{G}_T^h(\mathbf{u}_T^h, \mathbf{u}_{\partial T}^h) : \boldsymbol{\tau}_T^h &= \int_T \nabla \mathbf{u}_T^h : \boldsymbol{\tau}_T^h + \int_{\partial T} (\mathbf{u}_T|_{\partial T} - \mathbf{u}_T^h|_{\partial T}) \cdot \boldsymbol{\tau}_T^h|_{\partial T} \cdot \mathbf{n} && \forall \boldsymbol{\tau}_T^h \in S^h(T) \\ &= \int_T \nabla \mathbf{u}_T^h : \boldsymbol{\tau}_T^h + \int_{\partial T} \mathbf{u}_T^\perp|_{\partial T} \cdot \boldsymbol{\tau}_T^h|_{\partial T} \cdot \mathbf{n} && \forall \boldsymbol{\tau}_T^h \in S^h(T) \end{aligned} \quad (60)$$

using the divergence theorem and the fact that $\nabla \cdot \boldsymbol{\tau}_T^h \in U^h(T)$, one has :

$$\int_T \nabla \mathbf{u}_T^\perp : \boldsymbol{\tau}_T^h = \int_{\partial T} \mathbf{u}_T^\perp|_{\partial T} \cdot \boldsymbol{\tau}_T^h|_{\partial T} \cdot \mathbf{n} \quad (61)$$

such that :

$$\begin{aligned} \int_T \mathbf{G}_T^h(\mathbf{u}_T^h, \mathbf{u}_{\partial T}^h) : \boldsymbol{\tau}_T^h &= \int_T \nabla \mathbf{u}_T^h : \boldsymbol{\tau}_T^h + \int_T \nabla \mathbf{u}_T^\perp : \boldsymbol{\tau}_T^h && \forall \boldsymbol{\tau}_T^h \in S^h(T) \\ &= \int_T \nabla \mathbf{u}_T : \boldsymbol{\tau}_T^h && \forall \boldsymbol{\tau}_T^h \in S^h(T) \end{aligned} \quad (62)$$

which states that $\mathbf{G}_T^h(\mathbf{u}_T^h, \mathbf{u}_{\partial T}^h)$ is the orthogonal projection of $\nabla \mathbf{u}_T$ onto $S^h(T)$.

Reconstructed gradient. For any displacement pair $(\mathbf{v}_T^l, \mathbf{v}_{\partial T}^k) \in U^h(T) \times V^h(\partial T)$, the component $G_{T\theta\theta}(v_{Tr}, v_{\partial Tr})$ solves

$$\int_T 2\pi r G_{T\theta\theta}(v_{Tr}, v_{\partial Tr}) \tau_{T\theta\theta} = \int_T 2\pi r \frac{u_{Tr}}{r} \tau_{T\theta\theta} = \int_T 2\pi u_{Tr} \tau_{T\theta\theta} \quad \forall \boldsymbol{\tau}_T \in S(T) \quad (63)$$

In the radial and ordonal directions, i.e. $\forall i, j \in \{r, z\}$, the expression given in (16) is retrieved, and the component $G_{Tij}(v_{Ti}, v_{\partial Ti})$ solves

$$\int_T 2\pi r G_{Tij}(v_{Ti}, v_{\partial Ti}) \tau_{Tij} = \int_T 2\pi r \frac{\partial u_{Ti}}{\partial j} \tau_{ij} - \int_{\partial T} 2\pi r (u_{\partial Ti} - u_{Ti}|_{\partial T}) \tau_{Tij}|_{\partial T} n_j \quad \forall \boldsymbol{\tau}_T \in S(T) \quad (64)$$

Reconstructed higher order displacement. For any $\mathbf{d}_T^{k+1} \in D^h(T)$, the radial component w_{Tr}^{k+1} solves

$$\begin{aligned} \int_T 2\pi r \left(\sum_{i \in \{r,z\}} \frac{\partial w_{Tr}^{k+1}}{\partial i} \frac{\partial d_{Tr}^{k+1}}{\partial i} + \frac{w_{Tr}^{k+1}}{r} \frac{d_{Tr}^{k+1}}{r} \right) &= \int_T 2\pi r \left(\sum_{i \in \{r,z\}} \frac{\partial u_{Tr}}{\partial i} \frac{\partial d_{Tr}^{k+1}}{\partial i} + \frac{u_{Tr}}{r} \frac{d_{Tr}^{k+1}}{r} \right) \\ &+ \int_{\partial T} 2\pi r \sum_{i \in \{r,z\}} (u_{\partial Tr} - u_{Tr}|_{\partial T}) \frac{\partial d_{Tr}^{k+1}}{\partial i}|_{\partial T} n_i \end{aligned} \quad (65)$$

where the mean value condition is not needed on the radial component of the higher order displacement since the left hand side of the system described by (65) depends directly on the displacement unknown and not only on its gradient as in (66). The ordinate component w_{Tz}^{k+1} solves :

$$\int_T 2\pi r \sum_{i \in \{r,z\}} \frac{\partial w_{Tz}^{k+1}}{\partial i} \frac{\partial d_{Tz}^{k+1}}{\partial i} = \int_T 2\pi r \sum_{i \in \{r,z\}} \frac{\partial u_{Tz}}{\partial i} \frac{\partial d_{Tz}^{k+1}}{\partial i} - \int_{\partial T} 2\pi r \sum_{i \in \{r,z\}} (u_{\partial Tz} - u_{Tz}|_{\partial T}) \frac{\partial d_{Tz}^{k+1}}{\partial i} n_i \quad (66a)$$

$$\int_T 2\pi r w_{Tz}^{k+1} = \int_T 2\pi r u_{Tz} \quad (66b)$$

References

- [1] W. Reed, T. Hill, Triangular mesh methods for the neutron transport equation, Tech. rep., United States, IA-UR-73-479 INIS Reference Number: 4080130 (1973).
- [2] D. A. Di Pietro, J. Droniou, A. Ern, A Discontinuous-Skeletal Method for Advection-Diffusion-Reaction on General Meshes, SIAM Journal on Numerical Analysis 53 (5) (2015) 2135–2157. doi:10.1137/140993971.
URL <http://pubs.siam.org/doi/10.1137/140993971>